Supporting Information for

Fano Enhancement of SERS for Rapid Early Diagnosis of Coloretal Cancer

Tianxun Gong,[a] Zhenjiang Wei,[a] Libin Huang,[b] Yan Hong,[c] Yuan Li,[b] Ke-ling Chen,[b] Wen Huang,[a] Xiaojing Zhong,[d] Jinzhao He,[d] Ming-Yi Lee,[e] En-Chi Chang,[e] Kien Voon Kong,[e*] Xiaosheng Zhang,[a*] Zongguang Zhou[b*]

[a]State Key Laboratory of Electronic Thin Films and Integrated Devices, School of Electronic Science and Engineering (National Exemplary School of Microelectronics), University of Electronic Science and Technology of China, Chengdu, China.

[b]Laboratory of Digestive Surgery, State Key Laboratory of Biotherapy and Cancer Center, and Department of Gastrointestinal Surgery, West China Hospital, West China School of Medicine, Sichuan University, China.

[c]School of Materials and Energy, University of Electronic Science and Technology of China, Chengdu, China.

[d]Department of Internal Medicine-Neurology, Heyuan People's Hospital, China.

[e]Department of Chemistry, National Taiwan University, Taipei, 10617, Taiwan.

* Email: kvkong@ntu.edu.tw; zhangxs@uestc.edu.cn; zhou767@scu.edu.cn.

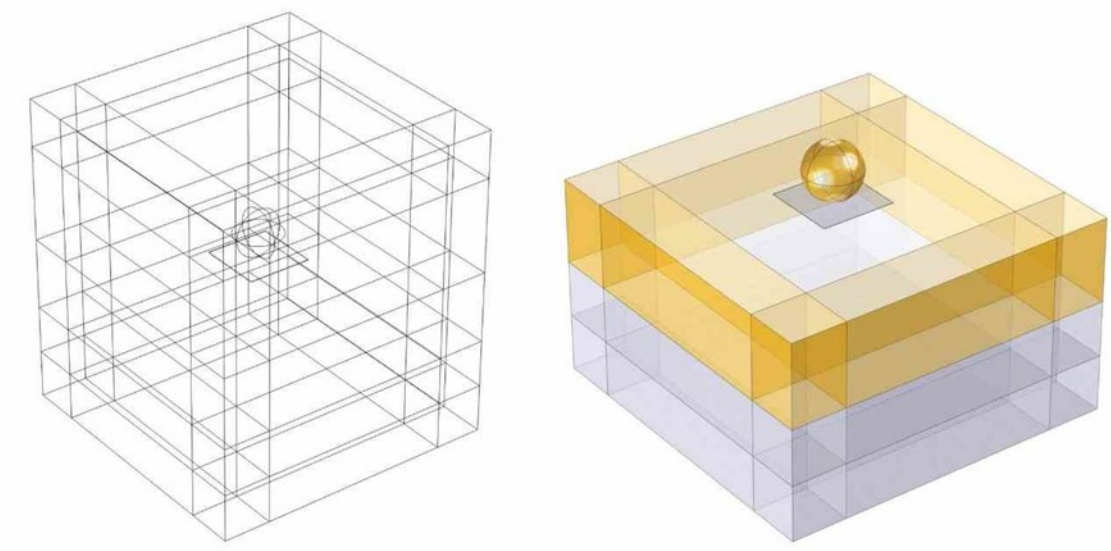

Figure S1. The simulation model

The simulation uses the electromagnetic field frequency domain calculation interface in the Wave Optics Module of COMSOL. This interface is used to solve the electromagnetic field distribution, charge distribution, and absorption-scattering-extinction spectra of the Raman sensing chip based on Fano resonance. The model is shown in Fig. S1, an Au-NS is placed on a dielectric layer, and below the dielectric layer is a silicon-based gold-coated substrate. The diameter D of the Au-NS ranges from 160 to 240 nm, the refractive index n_b of the dielectric layer is set to 1.4, the thickness of the gold coating on the substrate is 300 nm, the simulation wavelength ranges from 500 nm to 1000 nm, and the incident light angle is 0° (perpendicular to the xy plane). Specific parameters are shown in Table S1:

TABLE S1. Model Parameters

Name	Value
Physical geometry width	750 nm
PML thickness	150 nm
Air domain height	400 nm
Dielectric layer thickness	1 nm
Refractive index, air	1
Refractive index, dielectric layer	1.4
Incident polar angle in air	0
Incident field strength	1 MW/m²
Port power	$5.625e^{-7}$ W

In the electromagnetic field frequency domain calculation interface, the wave equation is:

$$\nabla \times (\nabla \times E) = k_0^2 \varepsilon_r E$$

The boundary is set to the Floquet periodic condition, which means that the solution on one side of the model structure of the Raman sensing chip based on Fano resonance is equal to the solution on the opposite side multiplied by a complex phase factor. This setting indicates that the model structure is not an individual entity but a repeating unit in an infinitely large plane, consistent with the actual experiment of fabricating large-scale Raman sensing chips based on Fano resonance.

In the numerical simulation, calculating the absorption, scattering, and extinction spectra is one of the challenges. First, the absorption, scattering, and extinction cross-sections of the simulation model must be determined. The expression for the scattering cross-section is:

$$\sigma_{SC} = \frac{1}{I_0} \iint (n \bullet S_{SC}) dS$$

S_{sc} is the scattered light intensity vector, n is the normal vector pointing outward from the inside of the nanosphere, and I_0 is the incident field strength (which can be set by the user). By performing a closed surface integral over the nanosphere, the expression for the absorption cross-section can be obtained, as shown below:

$$\sigma_{abs} = \frac{1}{I_0} \iiint Q dV$$

Q is the power loss density of the nanosphere. The extinction cross-section is the sum of the scattering cross-section and the absorption cross-section:

$$\sigma_{ext} = \sigma_{abs} + \sigma_{SC}$$

During modeling, two electromagnetic field frequency domain calculation interfaces were used. The first one solves the background field in the absence of the nanosphere, where the background field is undisturbed by the nanosphere and can serve as the input field for the second electromagnetic field frequency domain calculation interface. The second electromagnetic field frequency domain calculation interface includes the nanosphere as a scatterer, and the background field calculated by the first interface is used as the input. A surrounding perfectly matched layer (PML) is added to the model, which can absorb all the energy without reflection. The scattered field absorbed by the PML is the required scattered field.

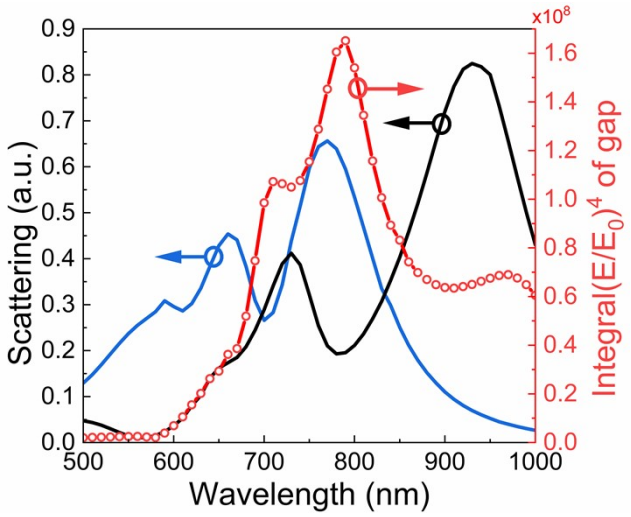

Figure S2. The scattering spectra of Au-NS substrate with diameter of 200 nm and Au thickness of 15 nm (black curve), and its' average electric-field at the nanogap (red curve). The blue curve corresponds to the scattering spectra of Au-NS substrate composed of an Au nanosphere with diameter of 200nm. The average electric-field enhancement is estimated from the volume average of nanogap with $|E/E0|^4$.

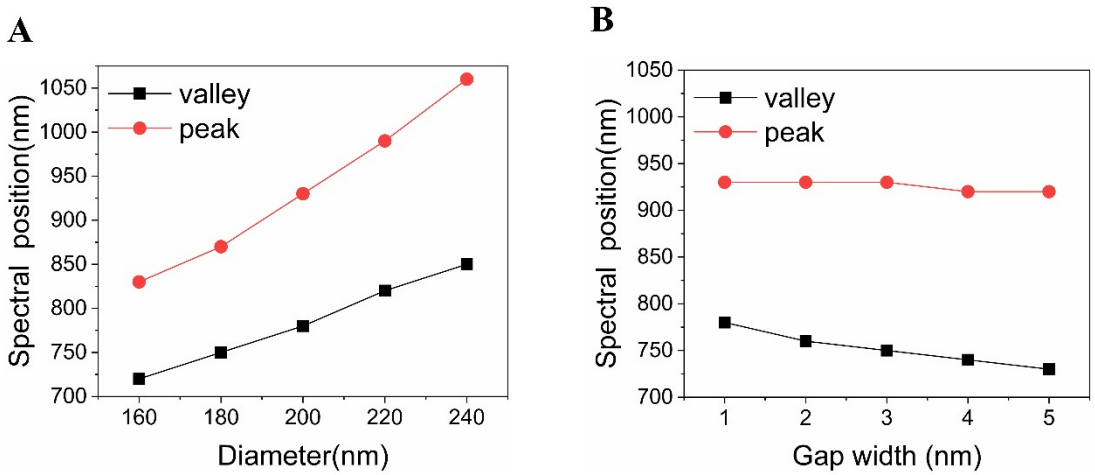

Figure S3. Influence of spacing and nanosphere diameter on Fano resonance. (A) Fano scattering valleys corresponding to different radius (black curve, the wavelength corresponding to the purple dotted line in Figure 2b) and the main scattering peak (red curve) changed with the radius. (B) Fano scattering valleys corresponding to different gap distances (black curve, the wavelength corresponding to the purple dotted line in Fig. 3L) and the main scattering peak (red curve) changed with the gap distance.

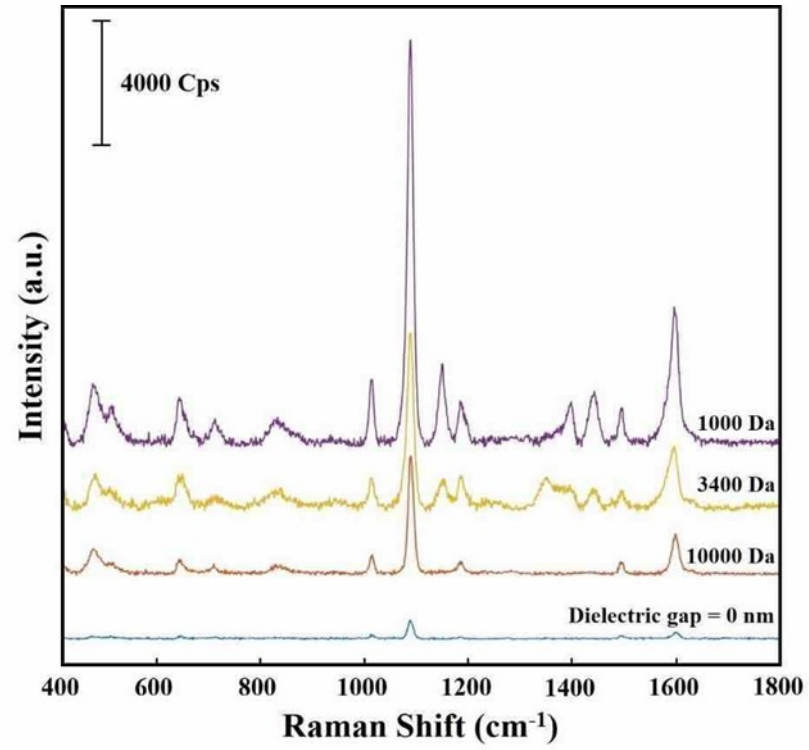

Figure S4. Raman intensity of 4-aminothiophenol on **Au-NS** substrate with PEG with different molecular weight.

As shown in Figure S3, the Raman enhancement of 4-aminothiophenol (5 μL, 1 mM) by the **Au-NS** substrate was tested under different molecular weights of PEG. It can be found that the **Au-NS** substrate with no PEG (0 nm gap) has the weakest enhancement on the Raman signal. The Raman intensity of PEG with a molecular weight of 1000 Da is the strongest. It can be concluded that as the length of PEG further increases, the gap between the nanospheres and the gold film increases, its Fano resonance becomes less obvious and the Raman enhancement effect becomes weaker and weaker. This conclusion corresponds to the conclusion of the numerical simulation.

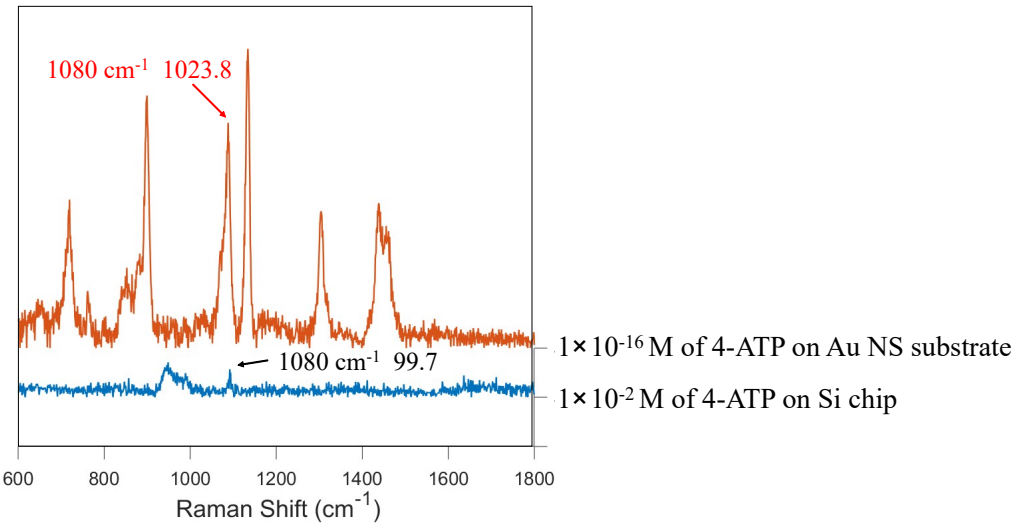

Figure S5. (A) Raman spectra of Au-NS substrate with 1×10^{-16} M of 4-ATP and Si chip with 1×10^{-2} M of 4-ATP. Raman spectra of were collected by Horiba iHR550 spectrometer using an excitation laser wavelength at 785 nm under ×100 objective lens. The laser power is ~2.7 mW, and the accumulation time is 1 s.

According to the above equation,

$$EF = \frac{I_{SERS}/C_{SERS}}{I_{RS}/C_{RS}}$$

while I_{SERS}=1023.8, C_{SERS}=1×10^{-16} M, I_{RS}=99.7, C_{RS}=1×10^{-2} M, the SERS enhancement factor of the Au-NS substrate is EF=1.03×10^{15}

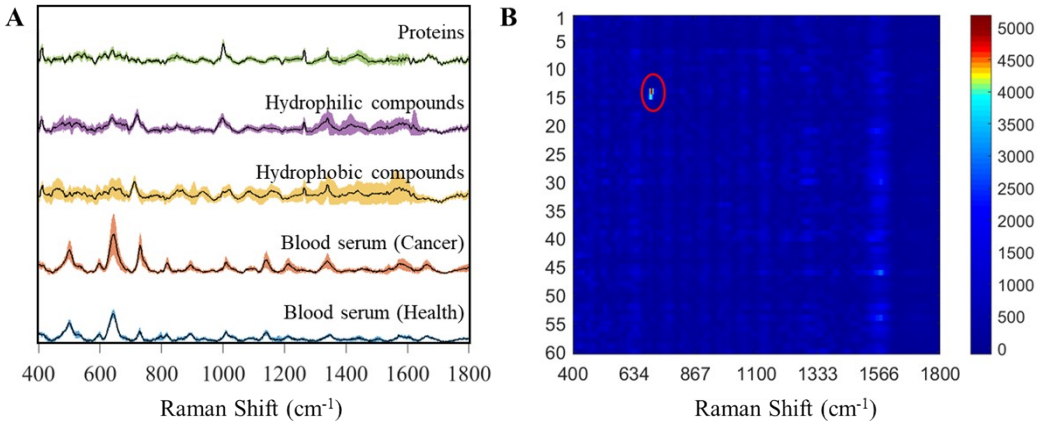

Figure S6. (A) Raman spectra of blood serum from cancer patients and health control, and different compounds from cancer patients' blood serum. (B) Heat map of the Raman spectra of all hydrophilic compounds from cancer patient's blood serum (compounds No. 1-60).

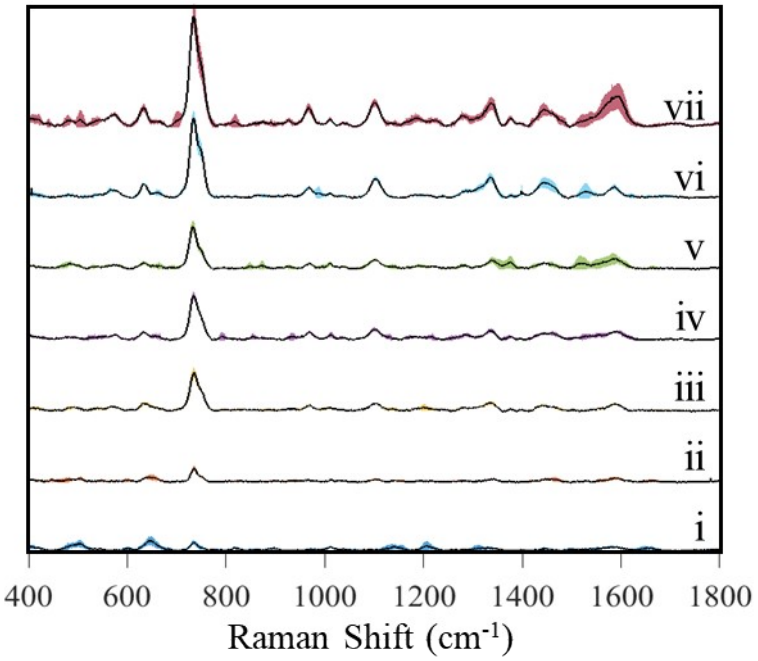

Figure S7. i. Raman spectra of cancer patient's blood serum. ii-vii. Raman spectra of cancer patient's blood serum mixed with hypoxanthine concentrations of 50 µM, 100 µM, 200 µM, 500 µM, 1 mM, correspondingly.

TABLE S2. Attempted assignments of major bands in Figure 4a that shows obvious difference between the cancer and health samples.

Shift (cm^{-1})	ΔInt.	Vibrational mode	Assignment	Health	Cancer
480	m	ν(S-S)	L - arginine	+	
599	w		Amide - VI		+
622	m	δ(C-C)	Phenylalanine	+	
648	m	δ(C-C)	Tyrosine	+	
726	s	ν(C-H)	Hypoxanthine	+	
741	m		Thymine	+	
838	m	Ring breathing	Tyrosine	+	
896	w	ν(C-C)	Proteins (α-helix conformation)		+
972	m		Hypoxanthine	+	
1029	m	δip (C-H)	Phenylalanine	+	
1091	m	ν(C-N)	d - Mannos	+	
1141	m	ν(C-C)	Lipid		+
1165	m	δip (C-H)	Tyrosine	+	
1262	s	δip (=CH)	Lipid		+
1307	m	δ (CH_2)	Collagen	+	
1435	m	δ (CH_2）	Collagen	+	
1484	w	δ (CH_2)	Lipid		+
1574	s	δ (C=C）	Tryptophan	+	

ν: stretching; δ: bending ; νs: symmetric stretching; ip: in plane

m: medium; s: strong; w: weak

+: Higher intensity

Table S3. Liquid chromatography conditions.

Keep time	Mobile phase Buffer A (%)	Mobile phase Buffer B (%)
0	5	95
2	5	95
48	25	75
53	40	60
57	60	40

60	5	95

Table S4. Non-targeted mass spectrometry detection flow gradient.

Keep time	Mobile phase Buffer A (%)	Mobile phase Buffer B (%)
0	99	1
2	99	1
3.5	80	20
17	20	80
17.5	1	99
19	1	99
19.1	99	1
22	99	1

Ionization mode (QE)	positive
Spray voltage (kV)	3.5 ESI+
Capillary temperature (℃)	275

Sheath gas flow rate (Arb)	35
Aux gas flow rate (Arb)	8
Mass range (m/z)	70-1050
Full MS resolution	70000
MS/MS resolution	17500
TopN	10
NCE/stepped NCE	15,30,45
Duty cycle (s)	~1.2